Electronic Supplementary Material for PCCP

SUPPORTING INFORMATION FOR

Using Electrical and Optical Tweezers to Facilitate Studies of Molecular Motors

Mark E. Arsenault[(a)], Yujie Sun[(b)], Haim H. Bau[(a)], Yale E. Goldman[(b),]*

[(a)]Department of Mechanical Engineering and Applied Mechanics and [(b)]Pennsylvania Muscle Institute, University of Pennsylvania, Philadelphia, PA, 19104

*email: goldmany@mail.med.upenn.edu

Movie S1: Brightfield/fluorescent movie of a myosin V-coated bead moving helically along an actin filament (1 fps)

Movie S2: Brightfield/fluorescent movie of a myosin X-coated bead moving helically along an actin filament (9 fps)

Image Processing Details:

Figure S1 depicts the mean positions of two stationary beads along the optical axis, z, estimated using the method described in the main article (Eq. 2), as a function of their actual positions. The calibration (comparison) bead was a third bead in the same 50 μm x 50 μm field of view. The typical variability in the estimated bead z-position was ~ 200 nm, which is larger than the incremental steps taken when collecting calibration data. Accordingly, we did not interpolate between successive calibration images when estimating a bead's z-position. The typical uncertainty in a bead's x- or y-position was ~ 50 nm, which increased as the brightfield lamp intensity was decreased. The lamp intensity was kept low enough to monitor an actin filament's position and stiffness by fluorescence but was still sufficient to calculate a bead's rotational pitch.

To verify the results obtained for the bead's position along the optical axis, we explored three other methods: (i) the radius of the outermost fitted Gaussian ring,

max([R_1 R_2]) (Eq. 1 in the main article) (ii) the zeroth moment of the light intensity's absolute deviation from background, m_0, and (iii) its second moment, m_2 (ref. 1),

$$m_0 = \sum_{i^2+j^2 \le w^2} \left| A(\bar{x}+i, \bar{y}+j) \right| \tag{S1}$$

$$m_2 = \frac{1}{m_0} \sum_{i^2+j^2 \le w^2} \left| A(\bar{x}+i, \bar{y}+j) \right| (i^2 + j^2) . \tag{S2}$$

In the above equations, A is a pixel's intensity, i and j are integers designating individual pixels, $\bar{x}$ and $\bar{y}$ are the pixel coordinates of the bead's center, and w is the outer radius of the bead's image.

m_0 corresponds to the absolute 'volume' of the intensity profile and m_2 it's radius of gyration-squared. For example, m_2 would approximate the standard deviation-squared of a single Gaussian peak. Figures S2 and S3 depict, respectively, m_0 and m_2 of a stationary bead's images as functions of its z location. Negative z is closer to the viewing objective (positioned below the focal plane). If a bead's excursions are restricted to either side of the extrema in Figs. S2 & S3, an accurate, single-valued determination of its z-position can be made from these moments. Notice that the z-range in Figs. S2 and S3 span 10 μm, and a 1 μm-diameter bead is only expected to explore ~ 1 μm along the optical axis when traveling along an actin filament that lies in the focal plane. The insets in Figs. S2-S4 expand the ~1 μm range that is explored by the bead of Fig. S5 (and Figs. 2a & 4 in the main article). The exact location of the focal plane is uncertain, so z = 0 was chosen to approximately coincide with the minimum in Fig. S2.

The outermost fitted Gaussian ring radius (Eq. 1 – main article) of a stationary bead is not as robust a measure of the z-position as m_0 and m_2. The diffraction patterns weaken near the focal plane, so fitting the radii becomes poorly constrained and sensitive to the

initial guess (Fig. S4)[2]. However, if a bead is restricted to locations corresponding to either side of the minimum, similarly to the cases of m_0 and m_2, the z-position can be readily determined.

These alternative methods' calibration curves pose ambiguities for beads near the focal plane. For the data presented in the main article, the same trends in z are produced using all four different methods (Figure S5 (top)). Figure S5 (bottom) shows the transverse position, x, as a function of its position along the filament, y, leading the z position data by approximately 90º.

[1] J. C. Crocker, D. G. Grier, Methods of Digital Video Microscopy for Colloidal Studies. *J. Colloid Interface Sci.,* 1996, **179**, 298-310.

[2] M. Speidel, A. Jonas, E. Florin, Three-dimensional tracking of fluorescent nanoparticles with subnanometer precision by use of off-focus imaging. *Opt. Lett.,* 2003 **28**: 69-71.

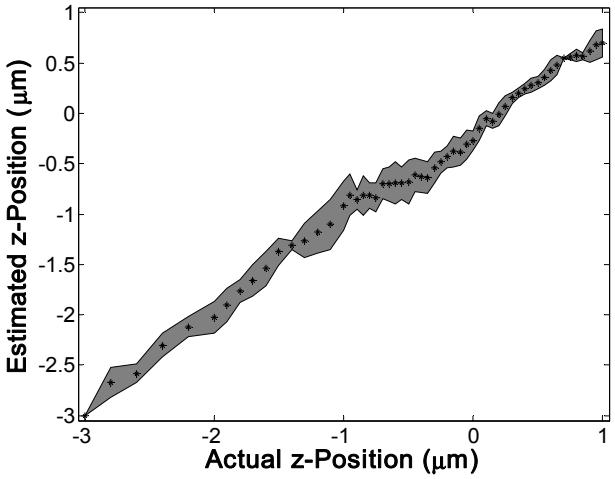

Figure S1. The estimated position of two stationary beads along the optical axis [mean ± standard deviation (gray-shaded) as determined from 20 images (10 images/bead) using Eq. 2 (main article)] depicted as a function of their actual position set by the position of a piezo-electric stage on the microscope. Negative values of z are closer to the viewing objective, below the focal plane.

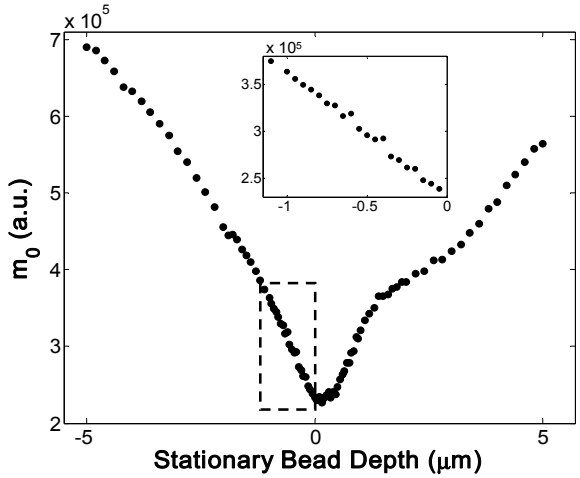

Figure S2. Zeroth moment, m_0, of a bead intensity profile, calculated using Eq. S1, plotted *vs.* z. The origin of the abscissa corresponds approximately to the focal plane. The inset details the range of depth explored by the bead presented in Fig. S5 (and Figs. 2a & 4 in the main article).

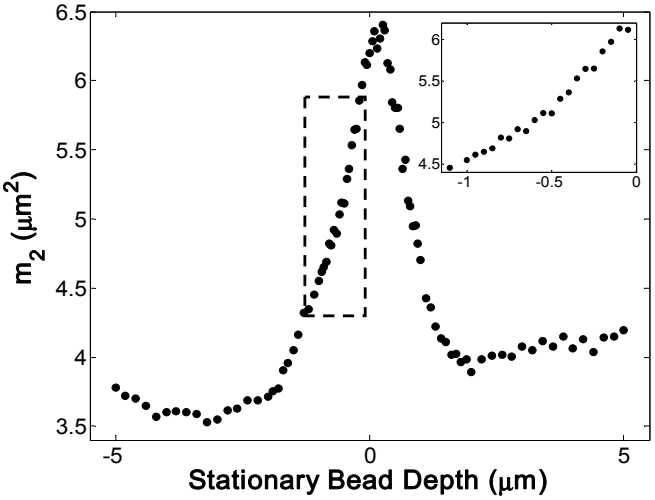

Figure S3. Second moment, m_2, calculated using Eq. S2, of the intensity profiles plotted *vs. z*. Origin and inset as in Fig. S2.

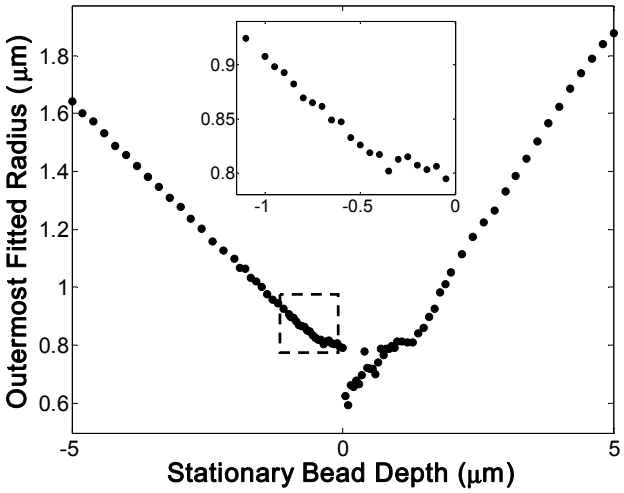

Figure S4. The radius of the outermost Gaussian ring (max([R_1 R_2])), fitted to a stationary bead's images using Eq. 1 (main article), plotted *vs. z*. Origin and inset as in Fig. S2.

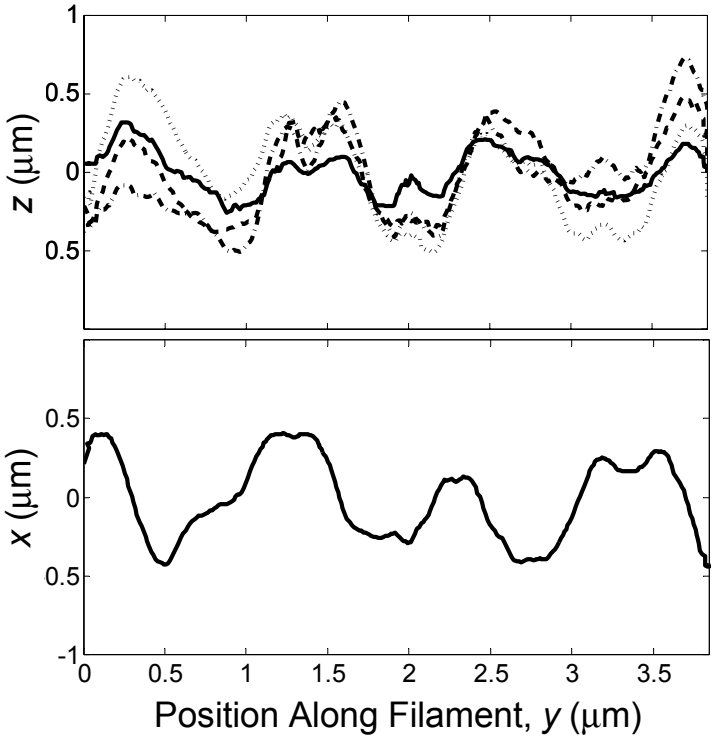

Figure S5. (**top**) A myosin-V coated bead's position along the optical axis, z, depicted as a function of its position along the filament, y, calculated using four different measures: (i) fit comparison (main article) (solid), (ii) zeroth moment, m_0 (dashed), (iii) second moment, m_2 (dotted), and (iv) radius of the outermost Gaussian ring (dash-dotted). (**bottom**) the transverse position, x, depicted as a function of its position along the filament. Its phase leads all four of the z-trajectories.